IEEE Access
Multidisciplinary | Rapid Review | Open Access Journal

Received April 3, 2019, accepted April 30, 2019, date of publication May 7, 2019, date of current version May 20, 2019.

Digital Object Identifier 10.1109/ACCESS.2019.2915354

An Enhanced Iterative Clipping and Filtering Method Using Time-Domain Kernel Matrix for PAPR Reduction in OFDM Systems

XIAORAN LIU, XIAOYING ZHANG, JUN XIONG, (Member, IEEE), FANGLIN GU, (Member, IEEE), AND JIBO WEI, (Member, IEEE)
Department of Electronic Science, National University of Defense Technology, Changsha 410073, China

Corresponding author: Jun Xiong (xj8765@ nudt.edu.cn)

This work was supported in part by the National Natural Science Foundation of China under Grant 61601477 and Grant 61601480, and in part by the Research Foundation of the National University of Defense Technology under Grant ZK17-03-13.

ABSTRACT Iterative clipping and filtering (ICF) is a straight-forward method for reducing the peak-to-average power ratio (PAPR) of signals in orthogonal frequency-division multiplexing (OFDM) system. Recently, convex optimization has been used to find the optimal filter coefficients that minimize the error vector magnitude (EVM) and meet the PAPR constraint. However, high-computation complexity may be incurred when solving the convex optimization problem. Therefore, we develop an efficient PAPR reduction method that uses the time-domain kernel matrix to generate the PAPR-reduction signal. Besides, we relax the assumption that the clipping noise is a series of uncorrelated parabolic pulses and apply the proposed method to more general cases. Based on the instantaneous observation of clipping noise, the proposed method constructs a simple time-domain kernel matrix and employs the curve fitting approach to optimize the corresponding scaling factors. The simulation results show that the proposed method can achieve very close performance to that using convex optimization in terms of both the PAPR reduction and EVM while the computational cost is reduced greatly. In addition, due to the decrease of iteration numbers and computational complexity, the proposed method is more efficient than some existing clipping and filtering methods.

INDEX TERMS OFDM, PAPR reduction, clipping and filtering, time-domain kernel, curve fitting.

I. INTRODUCTION

Orthogonal frequency division multiplexing (OFDM) is such a prominent technique that has been widely adopted in many wireless communication standards such as the 5th generation New Radio (5G NR), Long Term Evolution-Advanced (LTE-A), and IEEE 802.ax. However, the high peak-to-average power ratio (PAPR) of OFDM is a major drawback, which makes the signals sensitive to non-linear distortion of power amplifier (PA) [1]. Although this problem can be mitigated by yielding power back-off, it would result in the reduction of PA efficiency and the shrink of the coverage range [2].

Over the past decades, various PAPR-reduction techniques have been proposed in the literature, including tone reservation (TR) [3], selected mapping (SLM) [4], partial transmit sequence (PTS) [5], companding [6] clipping and filtering scheme [7]–[14], etc. These techniques can be divided into two main categories, distortionless techniques and signal distortion techniques [15]. Among all these existing techniques, the iterative clipping and filtering (ICF) method has received considerable research interest because it requires neither side information nor extra spectral resources and it presents possibly the simplest PAPR reduction scheme. During each iteration of ICF, the clipping procedure directly confines the amplitude of OFDM signal to a preset threshold and then the filtering procedure suppresses the consequent out-of-band emission. Nevertheless, since the filtering procedure results in peak regrowth, a number of iterations are usually required to achieve the desired PAPR reduction [7]. Besides, another problem of this method is that the in-band distortion caused by clipping has not been considered.

To address these problems, various modified methods have been proposed. In [8], a simplified clipping and filtering (SCF) method is proposed, in which the clipping noise is scaled to achieve the same PAPR reduction as that of ICF

The associate editor coordinating the review of this manuscript and approving it for publication was Maurizio Magarini.

with just one iteration. This is based on the analysis that the clipping noise generated in the first clipping and filtering iteration is approximately proportional to that obtained after several iterations. To reduce the computational complexity, the authors in [9] have designed a neural network to emulate the SCF signal pattern. Furthermore, a new approach that does not rely on clipping ratio has been proposed to minimize the number of iterations [16]. On the other hand, the in-band distortion is considered in [10] through the constrained error vector magnitude (EVM), which makes the clipped signal satisfy specific communications standards. In [11], the distortion on each tone of OFDM is limited, which can be regarded as a generalization of active constellation extend (ACE) [17]. The optimization method is further applied to minimize the EVM in [12], [13]. In [12], an optimized ICF (OICF) method is proposed to find the optimal frequency-domain filtering coefficients that can minimize the EVM. However, the drawback of this method is that solving a convex optimization problem results in very high computation complexity. To overcome this problem, the optimization problem in the original OICF method is transformed into an approximate form, which is called simplified OICF (SOICF) [13]. By using algebraic operations to approximately solve the optimization problem, the computation complexity can be significantly reduced. This method is further considered in an adaptive clipping fashion but the bit error ratio (BER) performance is then degraded [14]. In fact, the SOICF method is only useful for the case when the clipping threshold is large enough to make the clipping noise approximated as a series of uncorrelated parabolic pulses.

The clipping noise has been well investigated based on the level-crossing theory which is widely used for PAPR analysis [18] and clipping based PAPR reduction techniques [19]–[22]. In [19], the clipping noise is analyzed in both time and frequency domain. In [20], the amplitude of the filtered clipping noise is optimally scaled to approximate the amplitude of original clipping noise by using the least square algorithm. In [21], a curve fitting based TR method is proposed to directly generate the PAPR-reduction signal that approximates the waveform of clipping noise. In [22], the time-domain kernel matrix is used to suppress multiple pulses of clipping noise in one iteration. However, these methods designed for the approximation of clipping noise are mainly based on TR scheme which has much difference with the clipping and filtering scheme.

In this paper, an enhanced iterative clipping and filtering method is proposed to generate the PAPR-reduction signal by using the time-domain kernel matrix, which is called TKM-ICF. Our work is motivated by the fact that the clipping noise cannot be seen as a series of parabolic pulses when the PAPR threshold is relatively low. Since the PAPR-reduction signal is designed to approximate the clipping noise, the proposed method shows the capability of adapting to the change of clipping level. Firstly, we formulate a new optimization problem in which a time-domain kernel matrix is constructed and the corresponding scaling vector is optimized to generate the PAPR-reduction signal. Our analysis reveals that it is an equivalent form of the problem formulated in [12]. Furthermore, since the main energy of kernel is centralized in the half main-lobe width, the samples of clipping noise within correlation time of statistical process can be covered with a kernel vector. In this case, we can significantly simplify the time-domain kernel matrix and obtain an approximate and intuitive solution of this optimization problem with lower complexity. The simulation results demonstrate that the proposed method achieves near optimal performance in terms of EVM and PAPR reduction. In addition, comparing with the traditional SOICF method, we find that our method is more robust when setting low clipping threshold.

This paper is organized as follows. Section II briefly reviews the PAPR problem in OFDM system and the clipping/filtering scheme. In section III, we present the related theoretical analysis and propose the TKM-ICF method. Then simulations are performed in Section IV. The conclusion is drawn in Section V.

II. OFDM SYSTEM AND CLIPPING/FILTERING SCHEME

A. PAPR PROBLEM IN OFDM SYSTEM

In the OFDM system with N subcarriers, the data symbol $X(k)$ is modulated to the k-th subcarrier, where $k = 0, 1, \ldots, N-1$. The subcarrier spacing is $\Delta f = 1/T_s$, where T_s is the symbol period. Then the continuous-time OFDM signal $x(t)$ can be written as

$$x(t) = \frac{1}{\sqrt{N}} \sum_{k=0}^{N-1} X(k) e^{j2\pi kt/T_s}, \quad 0 \le t \le T_s \tag{1}$$

The PAPR of OFDM signal $x(t)$ is denoted as

$$\text{PAPR} = \frac{\max_{t\in[0,T_s)} |x(t)|^2}{P_{av}}, \tag{2}$$

where $P_{av} = E\{|x(t)|^2\} = E\{|X(k)|^2\}$ is the average power of $x(t)$. The discrete samples of $x(t)$ may also be used to compute the PAPR like (2) when the oversampling factor $L \ge 4$ [23]. The oversampled signal $x(n)$ can be efficiently computed by the LN-point inverse Fourier transform (IDFT) of the data symbols with zero-padding, which is expressed as

$$x(n) = \frac{1}{\sqrt{N}} \sum_{k=0}^{N-1} X(k) e^{j2\pi kn/LN}, \quad 0 \le n \le LN-1 \tag{3}$$

The performance of PAPR reduction is normally evaluated by the complementary cumulative distribution function (CCDF) which represents the probability that the PAPR of the OFDM symbol exceeds a predetermined threshold PAPR_0, i.e.

$$\text{CCDF} = \Pr(\text{PAPR} > \text{PAPR}_0), \tag{4}$$

where $\Pr(\cdot)$ denotes the probability function.

B. CLIPPING AND FILTERING METHOD

In the ICF method, the clipping and filtering operation are iteratively performed to suppress the peak regrowth. The clipped OFDM signal $\tilde{x}(n)$ can be denoted as

$$\tilde{x}(n) = \begin{cases} Ae^{j\theta(n)}, & |x(n)| > A \\ x(n), & |x(n)| \le A \end{cases} \tag{5}$$

where $\theta(n)$ is the phase of $x(n)$, and A is the clipping level. Note that A needs to be recalculated in each iteration according to the predefined clipping ratio (CR), which is defined as [1]

$$\gamma = \frac{A}{\sqrt{P_{av}}}. \tag{6}$$

Note that the amplitude clipping leads to in-band distortion and out-of-band radiation. Filtering is then employed to the clipped signal in frequency domain to eliminate the out-of-band radiation. The rectangular window is used for frequency-domain filter design in [7], which passes the in-band and rejects the out-of-band frequency components.

However, this simple design of filter leads to peak regrowth, in which numerous iterations are normally required in order to achieve the desired PAPR. Another disadvantage is that the in-band distortion is not taken into consideration. The EVM is generally applied to measure the in-band distortion, which is defined as [12]

$$\text{EVM} = \sqrt{\frac{\frac{1}{N}\sum_{k=0}^{N-1}\left|X(k)-\hat{X}(k)\right|^2}{\frac{1}{N}\sum_{k=0}^{N-1}|X(k)|^2}} = \frac{\left\|\boldsymbol{X}-\hat{\boldsymbol{X}}\right\|_2}{\|\boldsymbol{X}\|_2}, \tag{7}$$

where $\hat{\boldsymbol{X}}$ denotes the filtered symbols and $\|\cdot\|_2$ denotes the 2-norm.

In the OICF method [12], the filter is optimally designed to minimize the EVM at each iterations. The frequency-domain symbol after clipping is denoted as $\tilde{\boldsymbol{X}} = \left[\tilde{\boldsymbol{X}}_{in}; \tilde{\boldsymbol{X}}_{out}\right]$, where $\tilde{\boldsymbol{X}}_{in} = \left[\tilde{X}(0), \tilde{X}(1), \ldots, \tilde{X}(N-1)\right]^T$ is in-band component and $\tilde{\boldsymbol{X}}_{out} = \left[\tilde{X}(N), \tilde{X}(N+1), \ldots, \tilde{X}(LN-1)\right]^T$ is out-of-band component. Then the optimization problem with regard to the filter coefficients can be formulated as [15]

$$\min_{\boldsymbol{H}\in\mathbb{C}^N} \text{EVM} = \frac{\left\|\boldsymbol{X}-\hat{\boldsymbol{X}}\right\|_2}{\|\boldsymbol{X}\|_2} \tag{8a}$$

$$s.t.\ \hat{\boldsymbol{X}} = \tilde{\boldsymbol{X}}_{in} \odot \boldsymbol{H} \tag{8b}$$

$$\tilde{\boldsymbol{X}}_{out} = \boldsymbol{0}_{(N-1)L\times 1} \tag{8c}$$

$$\hat{x} = \text{IDFT}(\hat{\boldsymbol{X}})_{LN} \tag{8d}$$

$$\frac{\left\|\hat{x}\right\|_\infty}{\left\|\hat{x}\right\|_2/\sqrt{LN}} \le \sqrt{PAPR} = \gamma, \tag{8e}$$

where the operator $\odot$ denotes Hadamard product, $IDFT(\hat{\boldsymbol{X}})_{LN}$ represents a LN-point IDFT for zero-padded $\hat{\boldsymbol{X}}$, $\boldsymbol{H} \in \mathbb{C}^N$ is the frequency-domain filter coefficient vector and $\|\cdot\|_\infty$ is the ∞-norm of a vector. The constraints (8b) and (8c) represent the filtering procedure which weights the in-band component $\tilde{\boldsymbol{X}}_{in}$ using $\boldsymbol{H}$ and sets the out-of-band component $\tilde{\boldsymbol{X}}_{out}$ to zero. (8e) guarantees that the PAPR of OFDM signal can not exceed the predefined threshold.

Although the constraint (8e) is non-convex, it can be turned to a convex function by approximating $\left\|\hat{x}\right\|_2$ to $\|\tilde{x}\|_2$. Thus the problem (8) can be formulated as a convex one and solved as a second-order cone program (SOCP). Under the constraint of PAPR level, the OICF method can provide better EVM performance with fewer iteration times than traditional ICF method. However, when using large number of subcarriers, the computation complexity is prohibitively high, which motivates us to find a low-complexity ICF method.

III. THE PROPOSED TKM-ICF METHOD

In retrospect to the original clipping and filtering scheme, we find that the filtering in frequency domain requires an IFFT/FFT pair at each iteration. The filtering operation with complex value multiplication also leads to extra computation cost. Therefore, in order to avoid the frequency filtering, we will use an additive PAPR-reduction signal as the optimization parameter.

A. PAPR REDUCTION SIGNAL DESIGN

Instead of frequency-domain filtering of the clipped signal, the additive PAPR-reduction signal could be used as follows

$$\hat{\boldsymbol{x}} = \boldsymbol{x} - \boldsymbol{c} = \text{IDFT}\left(\boldsymbol{X} - \boldsymbol{C}\right)_{LN}, \tag{9}$$

where $\boldsymbol{c} = [c(0), c(1), \ldots, c(LN-1)]^T$ is the time-domain PAPR-reduction signal and $\boldsymbol{C} = [C(0), C(1), \ldots, C(N-1)]^T$ is the corresponding frequency-domain PAPR-reduction signal.

The clipping noise $f(n)$ is the consequence of amplitude clipping in (5), which is written as

$$f(n) = x(n) - \tilde{x}(n). \tag{10}$$

The clipping noise consists of several intermittent segments at which $|x(n)| > A$. Let P denote the number of clipping segments. Then $f(n)$ can be expressed as the combination of a series of clipping segments, i.e.,

$$f(n) = \sum_{i=1}^{P} f_i(n), \tag{11}$$

where $f_i(n)$ is the i-th clipping segment. We suppose that the i-th clipping segment arises at n_{si}, its maximum amplitude occurs at n_i and the duration time is N_{τ_i}(i.e., the number of non-zero values of $f_i(n)$).

It is obvious that the amplitude of signal would not exceed the PAPR constraint if PAPR-reduction signal $\boldsymbol{c}$ is equal to the clipping noise $\boldsymbol{f}$. Note that the frequency spectrum of clipping noise is distributed over the whole OFDM band, while the PAPR-reduction signal $\boldsymbol{c}$ is generated in band-limited system. That is, $\boldsymbol{c}$ hardly equals $\boldsymbol{f}$. in other words, we can only design $\boldsymbol{c}$ to approximate $\boldsymbol{f}$ as far as possible.

The clipping noise $\boldsymbol{f}$ is considered as a series of parabolic pulses in the SOICF method [13]. According to the positions of P pulses, the PAPR-reduction signal is generated as

$$\boldsymbol{c} = \sum_{n_i=n_1}^{n_P} \mu(n_i)\,\boldsymbol{p}[((n-n_i))_{LN}], \quad i = 1, \ldots, P, \quad (12)$$

where $\mu(n_i) = (|x(n_i)| - A)\,e^{j\phi(n_i)}$ denotes the scaling factor, $\boldsymbol{p} = [p(0), p(1), \ldots, p(LN-1)]^T$ is the time-domain kernel vector, and $\boldsymbol{p}[((n-n_i))_{LN}]$ represents the right circularly shifted sequence of $\boldsymbol{p}$ by n_i, such that its maximum value position matches to the pulse's max peak. The basic kernel vector is generated as

$$p(n) = \frac{1}{N}\sum_{k=0}^{N-1} e^{j2\pi nk/LN}, \quad n = 0, \ldots, LN-1, \quad (13)$$

in which the maximum value occurs at $n = 0$ and is normalized to 1.

The advantage of SOICF is that the computational complexity is reduced. But it is assumed that every clipping segment is approximately a parabolic pulse and has only one local maximum value, which greatly limits the generality of this method. In fact, such an assumption is frequently violated even for $CR = 6$dB [19], which implies that this method may fail to work when the target PAPR is required to be relatively low.

B. OPTIMIZATION PROBLEM REFORMULATION

From the previous subsection, we know that the SOICF method may become ineffective when the clipping noise has the envelope curve different from the parabolic pulse. It can be easily found that improving the degree of freedom in the design of PAPR-reduction signal can achieve better approximation to $\boldsymbol{f}$. Therefore, we construct a time-domain kernel matrix $\boldsymbol{M}$, which contains LN column vectors $\boldsymbol{p}_0, \boldsymbol{p}_1, \ldots, \boldsymbol{p}_{LN-1}$ generated by circularly shifting $\boldsymbol{p}$ to every sampling points of one OFDM symbol, i.e., $\boldsymbol{p}_l = \boldsymbol{p}[((n-l))_{LN}]$, $l = 0, 1, \ldots, LN$. The time-domain kernel matrix $\boldsymbol{M}$ can be written as

$$\boldsymbol{M} = \left[\boldsymbol{p}_0, \boldsymbol{p}_1, \ldots, \boldsymbol{p}_{LN-1}\right]_{LN\times LN}. \quad (14)$$

Then we scale the column vector of $\boldsymbol{M}$ by defining the scaling vector as

$$\boldsymbol{\beta} = [\beta_0, \beta_1, \ldots, \beta_{LN-1}]^T. \quad (15)$$

The PAPR-reduction signal is then expressed as

$$\boldsymbol{c} = \boldsymbol{M}\boldsymbol{\beta}. \quad (16)$$

Based on the linearity and circular-shift property of the DFT, the PAPR-reduction signal can be transformed in the frequency domain as

$$\begin{aligned} C(k) &= \mathrm{DFT}(\boldsymbol{M}\boldsymbol{\beta})_{LN} \\ &= \mathrm{DFT}\left(\sum_{d=0}^{LN-1} \beta_d \boldsymbol{p}_d(n)\right)_{LN} \\ &= \sum_{d=0}^{LN-1} \mathrm{DFT}\left(\beta_d \boldsymbol{p}_d(n)\right)_{LN} \\ &= \sum_{d=0}^{LN-1} \beta_d \mathrm{DFT}\left(\boldsymbol{p}\left[((n-d))_{LN}\right]\right)_{LN} \\ &= \sum_{d=0}^{LN-1} \beta_d e^{-j\frac{2\pi dk}{NL}} \mathrm{DFT}(\boldsymbol{p})_{LN} \\ &= \frac{1}{\sqrt{N}} \sum_{d=0}^{LN-1} \beta_d e^{-j\frac{2\pi dk}{NL}}, \end{aligned} \quad (17)$$

for $k = 0, 1 \ldots, N-1$. We define the (k, d) element of $N \times LN$ matrix $\boldsymbol{R}$ as $r_{kd} = \frac{1}{\sqrt{N}} e^{-j\frac{2\pi kd}{LN}}$. Thus, the PAPR-reduction signal in frequency domain can be expressed as

$$\boldsymbol{C} = \boldsymbol{R}\boldsymbol{\beta}. \quad (18)$$

Finally, we can reformulate the optimization problem in (8) by substituting the variable $\boldsymbol{\beta}$ for filtering coefficients $\boldsymbol{H}$, as given by

$$\min_{\boldsymbol{\beta}\in\mathbb{C}^{LN}} \quad \frac{\|\boldsymbol{R}\boldsymbol{\beta}\|_2}{\|\boldsymbol{X}\|_2} \quad (19a)$$

$$s.t. \left\|\boldsymbol{x} - \boldsymbol{M}\boldsymbol{\beta}\right\|_\infty \le \frac{\gamma\|\tilde{\boldsymbol{x}}\|_2}{\sqrt{LN}}, \quad (19b)$$

where the PAPR constraint (8e) is changed to a convex function as (19b) by following the same procedure in [12].

It can be found that the optimization objective (19a) is also a convex function because of $\boldsymbol{R}^T\boldsymbol{R} \succeq 0$. Thus it can also be seen as a SOCP and solved by some public softwares like CVX [24]. It is noteworthy that the solution to the optimization problem (19) can also make the $\boldsymbol{H} \odot \tilde{\boldsymbol{X}} = \boldsymbol{X} - \boldsymbol{R}\boldsymbol{\beta}$ solve the problem in (8), and vice versa. We can also find that when the constraint (19b) only considers one peak at $n = 0$ and $\boldsymbol{\beta}$ only contains one element β_0, this optimization problem will derive the same result as SOICF [13].

Although the optimal time-domain PAPR-reduction signal can be obtained by solving (19), we are interested in simplifying this problem and finding a more intuitive solution.

C. PROPOSED METHOD

Inspired by [22], we find that when the PAPR-reduction signal $\boldsymbol{c}$ is well designed though adjusting $\boldsymbol{\beta}$ that fits $\boldsymbol{c}$ to the clipping noise $\boldsymbol{f}$, the PAPR constraint (19b) could be satisfied. Meanwhile, the deterioration of EVM performance depends only on the power of PAPR-reduction signal. The block diagram of the proposed method is displayed in Fig. 1. According to the calculation of the clipping noise, the prestored time-domain kernel matrix is multiplied by the optimized scaling vector. To generate the scaling vector, we resort to curve fitting method that makes the waveform of the PAPR-reduction signal approximate the waveform of clipping noise.

To concentrate on the magnitude fluctuation of clipping noise, we define the positions of non-zero values

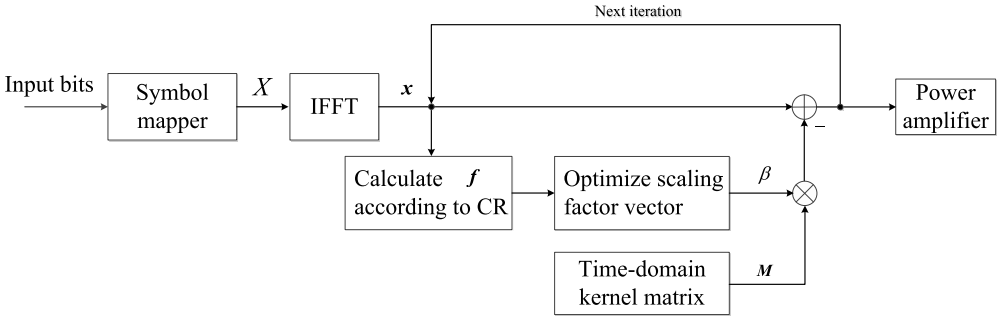

FIGURE 1. Block diagram of the OFDM transmitter with the proposed PAPR reduction method.

in i-th clipping noise segment $f_i(n)$ as the time index set $\mathcal{S}_i = \{n_0^i, n_1^i, \ldots, n_{N_{\tau_i}-1}^i\}$. Then we denote $\mathcal{S} = \mathcal{S}_1 \cup \mathcal{S}_2 \cup \cdots \cup \mathcal{S}_P$ and $N_\tau = \sum_{i=1}^{P} N_{\tau_i}$.

Then the problem of fitting $\boldsymbol{c}$ to $\boldsymbol{f}$ is equivalent to optimizing the vector $\boldsymbol{\beta}$ to minimize the Euclidean distance between the points $c(n)$ and $f(n)$ for $n \in \mathcal{S}$, which can be formulated as

$$\min_{\boldsymbol{\beta}} \sum_{n\in\mathcal{S}} |c(n) - f(n)|^2. \tag{20}$$

It can be found that (20) can be regarded as an intuitive and approximate form of (19) as analyzed above. We use $\hat{\boldsymbol{c}}$ and $\hat{\boldsymbol{f}}$ to represent the nonzero value of $\boldsymbol{c}$ and $\boldsymbol{f}$, respectively, i.e., $\hat{\boldsymbol{c}} = [\hat{\boldsymbol{c}}_1; \hat{\boldsymbol{c}}_2; \ldots; \hat{\boldsymbol{c}}_P]$, $\hat{\boldsymbol{c}}_i = [c(n_0^i), c(n_1^i), \ldots, c(n_{N_{\tau_i}-1}^i)]^T$, $\hat{\boldsymbol{f}} = [\hat{\boldsymbol{f}}_1; \hat{\boldsymbol{f}}_2; \ldots; \hat{\boldsymbol{f}}_P]$, $\hat{\boldsymbol{f}}_i = [f(n_0^i), f(n_1^i), \ldots, f(n_{N_{\tau_i}-1}^i)]^T$. Then the problem in (20) is rewritten as $\min_{\boldsymbol{\beta}} \left\| \hat{\boldsymbol{c}} - \hat{\boldsymbol{f}} \right\|_2^2$.

Note that there is no unique solution when the dimension of $\boldsymbol{\beta}$ is larger than that of $\hat{\boldsymbol{f}}$. In this case, we can simplify the time-domain kernel matrix by wiping out the vector $\boldsymbol{p}_d$ for $d \notin \mathcal{S}$, and only consider the curve fitting for the nonzero samples in clipping noise. In addition, samples in oversampled OFDM signal $x(n)$ may not be mutually independent. In fact, it has been shown that for cyclostationary process $x(t)$, the correlation coefficient of $x(t)$ and $x(t + \Delta t)$ is [19]

$$\rho_x(\Delta t) = \frac{\sin\left(\pi N \Delta t / T_s\right)}{N \sin\left(\pi \Delta t / T_s\right)} e^{-j\pi \Delta t / T_s}. \tag{21}$$

Here we can grossly define correlation time by the reciprocal of the bandwidth of the signals, i.e., $T_c \approx T_s/N$, by which the correlation of the stationary processes may rapidly diminish as the interval of observation exceeds T_c. Let $\Delta t = nT_s/LN$ for $0 \leqslant n \leqslant LN - 1$. Then we have

$$\left|\rho_x\left(nT_s/LN\right)\right| = \left|\frac{\sin\left(\pi n/L\right)}{N \sin\left(\pi n/LN\right)}\right| \approx \left|\frac{L \sin\left(\pi n/L\right)}{\pi n}\right|, \tag{22}$$

when n is small compared to N. As shown in (22), the samples within the range of L have large correlation, which proves that the clipping noise during the range of L is also correlated. Meanwhile, since the time-span of the main energy in time domain is significantly confined within the half main-lobe width T_s/N (which includes $L + 1$ samples for oversampled signal), it would be extremely inefficient to apply $\boldsymbol{p}$ to every sampling point in a clipping segment. Thus, the number of columns of kernel matrix $\boldsymbol{M}$ can be significantly reduced according to the segment duration N_{τ_i}.

When we lower the clipping level, the probability that more than one clipping pulses occur within the correlation time T_c will increase. That is, for one clipping segment, multiple local maximums could be found or the duration time frequently exceeds one half mainlobe width of $\boldsymbol{p}$. So considering the clipping noise in all cases, the time-domain matrix should be designed based on the instantaneous observation of clipping noise.

Suppose that the i-th clipping segment requires N_i kernel vectors, $\boldsymbol{p}_1^i, \boldsymbol{p}_2^i, \ldots, \boldsymbol{p}_{N_i}^i$ with circular shift $l_1^i, l_2^i, \ldots, l_{N_i}^i$, respectively, i.e.

$$\boldsymbol{p}_r^i = \boldsymbol{p}[((n - l_r^i))_{LN}], \quad r = 1, \ldots, N_i. \tag{23}$$

Next, we will determine the number of kernel vectors N_i and the value of circular shift l_r^i based on three cases of observation:

1) CASE 1

The first case is that the i-th clipping segment has only one local maximum and includes no more than L samples. Note that it is in accord with the assumption in [13], where the clipping segment can be regarded as a parabolic pulse. Then N_i is set to 1 and $\boldsymbol{p}_1^i$ is generated by circularly shifting $\boldsymbol{p}$ with $l_1^i = n_i$.

2) CASE 2

In the second case, more than one local maximum could be found in one clipping segment. Denote the number of local maximum in the i-th clipping segment as K_i. In this case, if the number of samples is less than $K_i \times L$ (the duration time is less than K_i times of correlation time T_c), N_i is then set as the number of all local maximums K_i among $f_i(t)$. The N_i kernel vectors are individually circular-shifted by the positions of K_i local maximums.

3) CASE 3

In the third case, the number of samples is greater than the $K_i \times L$. For example, if there is only one local maximum and the duration time of $f_i(t)$ is larger than the correlation time T_c, then the clipping segment cannot be covered within just one kernel vector. In this case, the number of vectors in kernel matrix for i-th clipping segment is calculated by $N_i = \lceil N_{\tau_i}/L \rceil$, where $\lceil \cdot \rceil$ denotes the ceiling function. Suppose that the segment duration is equally divided into N_i intervals, each of which has $(N_{\tau_i} - 1)/N_i$ samples. Meanwhile, the rising slope at the begin of segment and the falling slope at the end of segment are considered to jointly occupy one interval. In this way, the kernels are evenly spaced to be allocated in the duration of clipping segment. Thus the corresponding circular-shift value l_r^i is calculated by

$$l_r^i = n_{si} + \text{Round}(\frac{N_{\tau_i} - 1}{N_i}(r - \frac{1}{2})), \tag{24}$$

where Round$(\cdot)$ is to round off to the nearest integer. The first item is the starting position of the i-th clipping segment and the second item is the internal offset of the r-th kernel vector. Using (24) in (23), we can obtain N_i kernel vectors.

The amount of kernel vectors for each clipping segment is given by $N_p = \sum_{i=1}^{P} N_i$. We can redefine a reduced time-domain kernel matrix $\boldsymbol{M}_p$ which contains all the kernel vectors generated for each segment

$$\boldsymbol{M}_p = \left[\boldsymbol{p}_1^1, \ldots, \boldsymbol{p}_{N_1}^1, \boldsymbol{p}_1^2, \ldots, \boldsymbol{p}_{N_2}^2, \ldots, \boldsymbol{p}_{N_P}^P\right]_{LN \times N_p}. \tag{25}$$

The corresponding scaling factor vector is $\boldsymbol{\beta}_p = [\beta_1^1, \ldots, \beta_{N_1}^1, \beta_1^2, \ldots, \beta_{N_2}^2, \ldots, \beta_{N_P}^P]$. In order to focus on the non-zero value of $\boldsymbol{f}$, we denote $\hat{\boldsymbol{c}} = \hat{\boldsymbol{M}}_p \boldsymbol{\beta}_p$, where $\hat{\boldsymbol{M}}_p$ is a $N_\tau \times N_p$ matrix. The optimal $\boldsymbol{\beta}_p^*$ in (20) is the minimal norm least squares solution of the overdetermined linear equations

$$\hat{\boldsymbol{M}}_p \boldsymbol{\beta}_p - \hat{\boldsymbol{f}} = \boldsymbol{0}. \tag{26}$$

Since the column vectors of $\hat{\boldsymbol{M}}_p$ are uncorrelated, the rank of $\hat{\boldsymbol{M}}_p$ is N_p and smaller than N_τ. Thus, the equation (26) has a unique solution

$$\boldsymbol{\beta}_p{}^* = (\hat{\boldsymbol{M}}_p^H \hat{\boldsymbol{M}}_p)^{-1} \hat{\boldsymbol{M}}_p^H \hat{\boldsymbol{f}}. \tag{27}$$

The complexity of calculating the solution in (27) depends on the dimension of $\hat{\boldsymbol{M}}_p$. Because of the weak correlation of each clipping segment, we can further split the matrix $\hat{\boldsymbol{M}}_p$ into P low-dimension sub-matrices by independently considering the curve fitting in the i-th clipping noise segment, i.e.,

$$\min_{\boldsymbol{\beta}_i} \left\| \hat{\boldsymbol{c}}_i - \hat{\boldsymbol{f}}_i \right\|_2^2, \quad i = 1, 2, \ldots, P. \tag{28}$$

where $\hat{\boldsymbol{c}}_i$ can be expressed by $\hat{\boldsymbol{M}}_p^i \boldsymbol{\beta}_p^i$ and $\hat{\boldsymbol{M}}_p^i$ is a $N_{\tau_i} \times N_i$ matrix. Similar as (27), the solution in (28) can be obtained as

$$\boldsymbol{\beta}_p^{i}{}^* = (\hat{\boldsymbol{M}}_p^{i}{}^H \hat{\boldsymbol{M}}_p^i)^{-1} \hat{\boldsymbol{M}}_p^{i}{}^H \hat{\boldsymbol{f}}_i. \tag{29}$$

To ensure the PAPR constraint, we further modifies the solution in (28) by comparing the maximum value of clipping segment to that of the approximated signal. The modified solution is calculated as $\alpha_i \boldsymbol{\beta}_p^i$, where

$$\alpha_i = \frac{f_i(n_i)}{\|\hat{\boldsymbol{M}}_p^i \boldsymbol{\beta}_p^{i}{}^*\|_\infty}. \tag{30}$$

Particularly, for the case 1 that only one kernel vector is required (i.e., $N_i = 1$), β_p^i can be directly obtained by

$$\beta_p^i = f_i(n_i). \tag{31}$$

Since the scaling factor is set to the maximum of the clipping segment, we set $\alpha_i = 1$ as a constant.

Then we replace the calculated $\alpha_i \boldsymbol{\beta}_p^i$ for the corresponding $\beta_n(n = l_1^i, \ldots, l_{N_i}^i)$ of $\boldsymbol{\beta}$ and insert zero into the remainder of $\boldsymbol{\beta}$. In order to save computation cost, the PAPR-reduction signal is firstly generated in frequency domain [13], which can be obtained by (18). By converting $\boldsymbol{C}$ to the time domain, the iteration output signal can be expressed as

$$\hat{\boldsymbol{x}} = \boldsymbol{x} - \text{IDFT}(\boldsymbol{R}\boldsymbol{\beta})_{LN}. \tag{32}$$

Algorithm 1 The TKM-ICF Method

Initialization:

Set up the clipping ratio and the maximum number of iterations.

Generate the basic kernel vector $\boldsymbol{p}$ by (13).

Runtime:

1: Modulate OFDM signal $\boldsymbol{x}$ in time domain with oversampling factor L.
2: Calculate the average power P_{av} and set the clipping threshold A using (6).
3: Calculate the clipping noise $\boldsymbol{f}$ using (10).
4: For each clipping segments, generate the kernel vectors using (23) according to the three cases. Calculate $\alpha_i \boldsymbol{\beta}_p^i$ using (29), (30), and (31).
5: Calculate the PAPR-reduction signal $\boldsymbol{C}$ in frequency domain by (18). Transform $\boldsymbol{C}$ into time domain and update the OFDM signal $\boldsymbol{x}$ as (32).
6: If $\|\boldsymbol{x}\|_\infty \leq A$ or the maximum iteration number is reached, go to step1 and get new data to process the next OFDM symbol. Otherwise, go to step 2 to proceed the next iteration.

The proposed method is summarized in Algorithm 1. In order to further explain our proposed method, Fig. 2 shows the examples of time-domain observation of clipping noise for an OFDM system with oversampling factor $L = 8$. The PAPR-reduction signals generated by Algorithm 1 are presented to illustrate the curve fitting procedure. The corresponding kernel vectors are scaled and superimposed on each other to constitute the PAPR-reduction signal. For comparison, the optimal PAPR-reduction signals are obtained by solving convex optimization problem in (19). It can be seen that the clipping noise is classified into the three cases

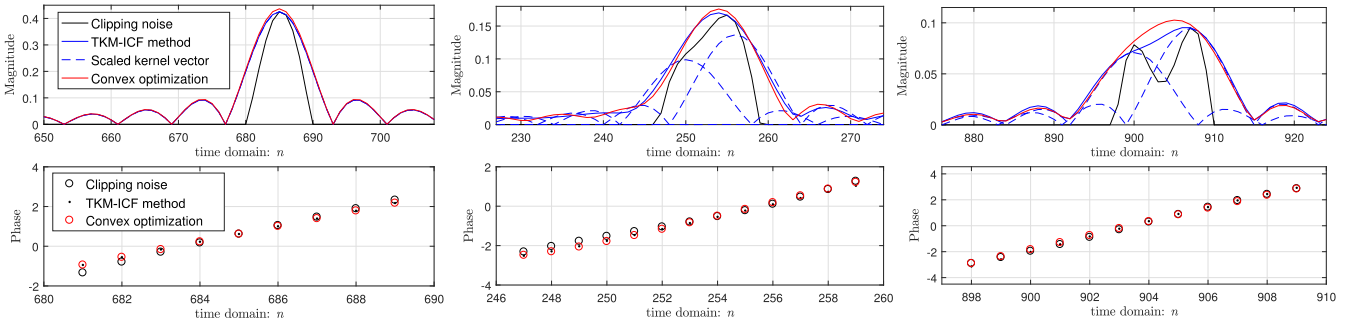

(a) Case 1 (b) Case 2 (c) Case 3

FIGURE 2. Examples of the clipping noise for three cases as illustrated in section III-C, and the PAPR-reduction signals generated by our proposed method and convex optimization method. (a) Case 1. (b) Case 2. (c) Case 3.

as illustrated above. For case 1, the clipping noise can be enveloped in one kernel vector. From the plots of amplitude and phase, the proposed method generates approximately identical PAPR-reduction signal to the convex optimization method. From Fig. 2(b) and Fig. 2(c), multiple kernel vectors are used to perform curve fitting as analyzed in case 2 and 3. The PAPR-reduction signals generated by the proposed method and convex optimization both have approximate envelope to the clipping noise, which infers that the clipping noise can be nearly canceled out. We also note that in case 1, the clipping segment can be assumed as a parabolic pulse. In this case, our proposed method is equivalent to the SOICF method, which implies that SOICF is a special case of our proposed method. However, the SOICF method cannot tackle case 2 and 3 since this assumption is no longer valid.

D. COMPLEXITY COMPARISON

In the Algorithm 1, since the basic kernel vector can be stored in advance and step 1-2 are the regular operations for the clipping and filtering scheme, we can ignore the computation cost before step 3.

In step 3, the complexity of calculating the clipping noise $f(n)$ by using (10) is $\mathcal{O}(LN)$. In step 4, the calculation of scaling factors includes the inverse and multiplication of matrix. The complexity of (27) is $\mathcal{O}(N_p^2 N_\tau)$, where N_p and N_τ determine the dimensions of $\hat{\boldsymbol{M}}_p$. By splitting the matrix $\hat{\boldsymbol{M}}_p$ into P sub-matrices, only for those cases that have more than one kernel vectors do we need to calculate the (29). The complexity for the case of $N_i > 1$ is accordingly reduced to $\mathcal{O}(N_i^2 N_{\tau_i})$. Note that N_i, N_{τ_i} and P are random variables. Assume that i-th clipping segment occurs in $(0, \Delta t)$. Then the probability of N_i can be estimated as the probability of N_i up-crossing pulses that occur within correlation time. It is written as [19, Equation (66)]

$$\Pr(N_i > m) = 1 - \sum_{v=0}^{m} \frac{(\lambda_A \Delta t)^v e^{-\lambda_A \Delta t}}{v!}, \tag{33}$$

where $\lambda_A = \sqrt{\frac{\pi}{3}}\gamma \frac{N}{T_s} e^{-\gamma^2}$ and $\Delta t = nT_s/N$. It implies that $\Pr(N_i > m)$ is independent to N and depends on CR. In the OFDM system with $N = 128$, $CR = 5.5$dB, we have the probability $\Pr(N_i > 0) \approx 0.2209$, $\Pr(N_i > 1) \approx 0.0264$ and $\Pr(N_i > 2) \approx 0.0022$. We can see that the probability drops rapidly as m increases, such as $\Pr(N_i = 2) \gg \Pr(N_i > 2)$. Then we suppose that in most cases N_i equals 2 and N_{τ_i} is set to its maximum value $2L$. Besides, from [18, Equation (14)], we know that the random variable P is dependent on CR and N. The expectation of P reaches its maximum when $\gamma = 0$, which can be calculated as $\bar{P} \approx 0.64N$. So the upper bound of computational complexity of (29) is estimated as $\mathcal{O}(8L \times 0.64N)$. In step 5, the computation of $\boldsymbol{C}$ using (18) is the same as DFT. Since the number of nonzero values in $\boldsymbol{\beta}$ is generally small as analyzed above, the inputs of the DFT are sparse. Therefore, the wavelet transform can be applied to this sparse signal [25], which only requires $\mathcal{O}(LN)$ complexity. Besides, the final output needs $\mathcal{O}(LNlog_2LN)$ complexity for the IDFT. As a result, the computational complexity of the proposed method is estimated as $\mathcal{O}(7.12LN + LNlog_2LN)$ in a single iteration. Because in most practical applications L is far less than N, the overall complexity of the proposed method is mainly determined by the IDFT.

The OICF method mainly includes two steps, i.e. solving the optimization problem and using an IDFT, which leads to $\mathcal{O}(N^3 + LNlog_2(LN))$ computation complexity [12]. Because of $L \ll N$, the complexity of OICF is much higher than the proposed method. For the SOICF method, most of the steps are similar to the proposed method. The computation of scaling factors in (12) is easier than the proposed method, which has the same operation as (31) [13]. However, due to the inevitable FFT operation, the saving of computation cost for SOICF is relatively small. As for the traditional ICF method [7], an FFT/IFFT pair is required in each iteration, leading to $\mathcal{O}(2 \times LNlog_2LN)$ complexity. Also, the frequency filtering in ICF have $\mathcal{O}((L-1)N)$ complexity. Therefore, the whole computational complexity is estimated as $\mathcal{O}((L-1)N + 2LNlog_2LN)$. The computation complexities of the TKM-ICF, OICF and ICF method are compared in Table 1. We can see that the OICF method has the highest computational cost due to the use of optimization tool. The complexities of proposed method and traditional ICF method are similar, which primarily depend on the IDFT/DFT operation. Since the proposed method only has one IDFT in

TABLE 1. Complexity comparison of the proposed TKM-ICF, OICF, and classical ICF methods.

Algorithm	Computational Complexity
TKM-ICF	$\mathcal{O}(7.12LN + LNlog_2LN)$
OICF	$\mathcal{O}(N^3 + LNlog_2(LN))$
ICF	$\mathcal{O}((L-1)N + 2LNlog_2LN)$

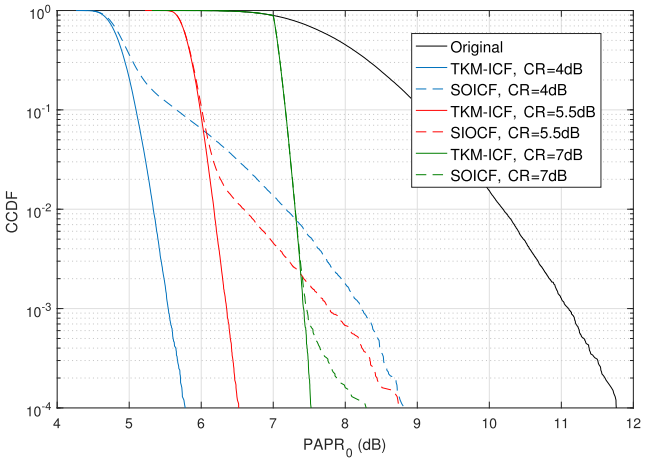

FIGURE 3. PAPR reduction performance of SOICF and TKM-ICF with different clipping ratio for $N = 128$ and QPSK modulation.

each iteration, the complexity of TKM-ICF is lower than that in ICF.

IV. SIMULATION RESULTS

To evaluate the performance of the proposed method, we present simulation results in this section. A typical OFDM system with $N = 128$ subcarriers and $L = 4$ oversampling is considered in our simulation. We compare the proposed algorithm with the SOICF [13], OICF [12], ICF [7] and SCF [8] methods.

In Fig. 3, we compare the performance of PAPR reduction between the SOICF and TKM-ICF methods with one iteration for CR $= 4, 5.5, 7$dB, respectively. When the desired PAPR is set to 7dB, the SOICF and TKM-ICF methods can achieve almost the same PAPR performance, since most of clipping segments include only one local maximum and can be approximated as a parabolic pulse. Nonetheless, the deviation happens when the PAPR is larger than 7.5dB. The curve of the SOICF method gradually deviates from that of the TKM-ICF method when the CCDF of PAPR is lower than 10^{-3}. Furthermore, when we set a lower clipping level, such as CR $= 4$ or 5.5dB, the difference of performance between the SOICF and TKM-ICF methods is increasingly enlarged. It implies that the assumption of parabolic pulse is reasonable only for CR $\rightarrow \infty$. This inference can be proven by using (33) as well, which shows the probability that two or more up-crossing pulses occur within a time interval will increase as the CR goes down. We can see that the TKM-ICF method properly adapts to the changes of CR and achieves better PAPR reduction performance.

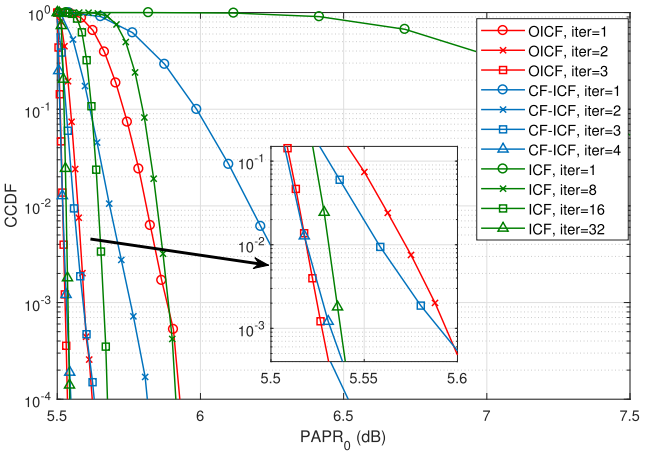

FIGURE 4. PAPR reduction performance of TKM-ICF, OICF, and ICF for $N = 128$ and QPSK modulation.

The proposed method is further compared with the OICF and ICF methods, when CR $=$ 5.5dB. Fig. 4 depicts the CCDF of PAPR for modified signal using OICF (for 1, 2 and 3 iterations), modified signal using traditional ICF (for 1, 8, 16 and 32 iterations), and modified signal using TKM-ICF (for 1, 2, 3 and 4 iterations). It can be seen that each method requires several iterations to reach the target PAPR threshold. The results of OICF method presented here can be seen as the optimal performance of PAPR reduction. For the TKM-ICF method, when the number of iterations is 4, the CCDF curve achieves a sharp fall at the desired PAPR and has no difference to that of the OICF method with 3 iterations. On the other hand, the traditional ICF method usually needs much more iterations to gradually converge at the target PAPR. After 32 iterations, the PAPR reduction level achieved by ICF is close to the desired PAPR. According to the complexity analysis above, in order to achieve the ideal performance, the OICF method costs $3 \times \mathcal{O}(N^3)$ computational complexity, and ICF needs at least 32 times IFFT/FFT pair operation resulting in $32 \times \mathcal{O}(2LNlog_2(LN))$ computational complexity. Nevertheless, the proposed method with 4 iterations only costs $4 \times \mathcal{O}(LNlog_2(LN))$ computational complexity, which is far more efficient than the other methods.

The performance of PAPR reduction of TKM-ICF, with different number of subcarriers, is performed in Fig. 5. The number of subcarriers is 256, 512, 1024, and 2048, respectively, with clipping ratio 5.5 dB and 16-QAM modulation. It can be observed that when the proposed method is executed once, the PAPR reduction in Fig. 5 is 5, 5.11, 5.2 and 5.28 dB, respectively, for 256, 512, 1024, and 2048 subcarriers, at CCDF $= 10^{-4}$. After three iterations, all the CCDF curves achieve a sharp fall nearly at the desired PAPR threshold. The performance analysis indicates that the TKM-ICF method is feasible for OFDM systems with different subcarriers.

Table 2 lists the EVM performance of the TKM-ICF method compared with that of the OICF, ICF, and SCF methods. The CR is fixed to 5.5dB for the TKM-ICF and OICF

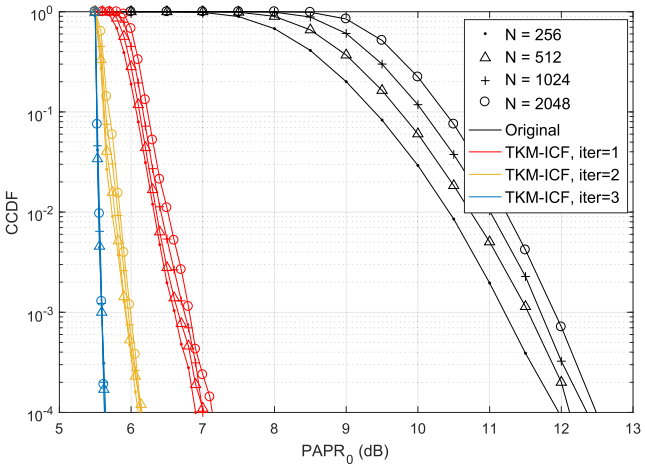

FIGURE 5. PAPR reduction performance with different subcarrier numbers (N =256, 512, 1024, and 2048) and 16-QAM modulation.

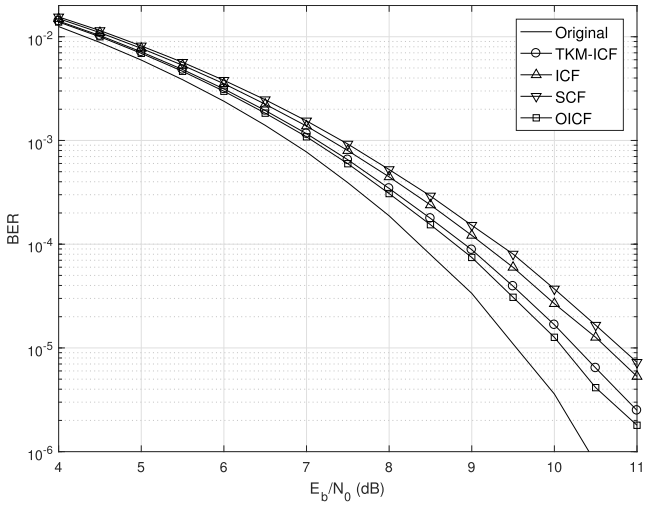

FIGURE 6. BER performance of TKM-ICF, OICF, ICF, and SCF methods with $N = 128$ and QPSK modulation over AWGN channel.

TABLE 2. Performance comparison of TKM-ICF, OICF, ICF, and SCF methods.

Algorithm	Iteration	Clipping Ratio (dB)	Average PAPR(dB)	RMS-EVM(%)
TKM-ICF	4	5.5	5.51	9.58
OICF	3	5.5	5.51	9.24
ICF	4	4.9	5.51	10.31
SCF		4.1	5.51	11.52

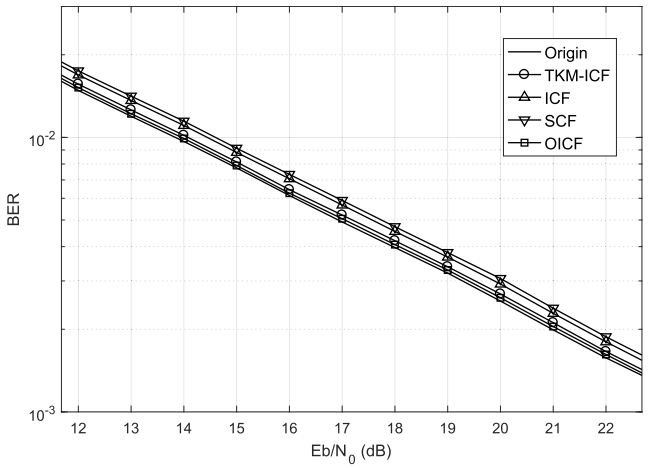

FIGURE 7. BER performance of TKM-ICF, OICF, ICF and SCF methods with $N = 128$ and QPSK modulation over Rayleigh fading channel.

methods. This target CR is achieved by 3 and 4 iterations for the OICF and TKM-ICF methods, respectively. For the ICF and SCF methods, the CR is deliberately selected such that the average PAPR achieved by these methods are equal to that of the proposed method with no more than 4 iterations. We can see that the OICF method has optimal EVM performance as expected. The EVM difference between the OICF and TKM-ICF methods is only 0.34%. The other two methods lead to more than 10% EVM, which can give rise to severe deterioration of demapping in receiver.

Fig. 6 and Fig. 7 provide the comparison of the uncoded BER performance with different clipping and filtering methods over additive white Gaussian noise (AWGN) channel and Rayleigh fading channel, respectively. Rayleigh channel is assumed to be quasi-static frequency selective and channel estimation is perfectly known at the receiver. The simulation parameters are the same as in Table 2 in order to show the effects of in-band distortion of different methods. The unclipped OFDM signal without PAPR reduction technique is considered as the reference. It can be observed from Fig. 6 that the BER curves of these methods are always worse than the ideal results. This is because the clipping procedure causes signal distortion. However, comparing the BER curve of the TKM-ICF method with other methods, we can see that the TKM-ICF method has a slight difference of BER performance with the OICF method and causes less SNR loss than the ICF and SCF methods at given BER requirement. For example, for the BER level of 10^{-5}, the ICF and SCF methods yield more than 0.6dB SNR loss compared with the OICF method, while the performance difference between the TKM-ICF and OICF methods is about 0.1dB. It demonstrates that the proposed the TKM-ICF method leads to less in-band-distortion than that of the ICF and SCF methods, and achieves similar performance to the OICF method. From Fig. 7, we can see that, in comparison with AWGN channel case, BER performance is obviously degraded when Rayleigh fading channel is considered. However, the proposed method is still better than the ICF and SCF methods and has similar BER performance to the OICF method. It should be noted that the computation complexity of OICF is prohibitively high, while the TKM-ICF method has much lower computation complexity than OICF.

Finally, to compare the out-of-band radiation, we consider passing the PAPR-reduced signal through a solid-state power amplifier (SSPA). The input/output model of SSPA can be

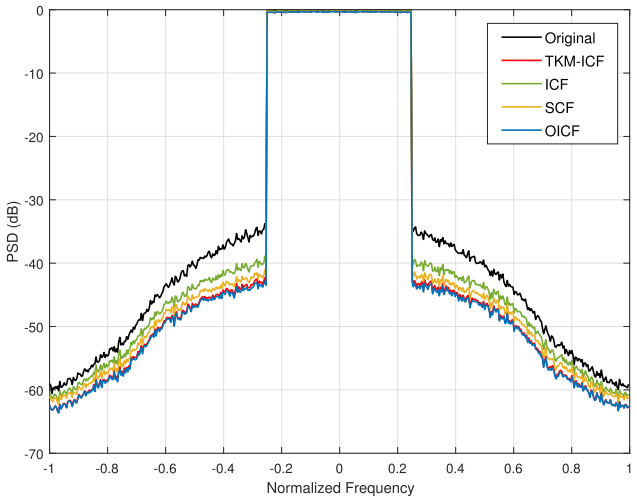

FIGURE 8. Out-of-band radiation comparison of OFDM signals with TKM-ICF, OICF, ICF, and SCF through SSPA model, with parameter $v = 3$ and $q = 1$dB.

written as [1]

$$s_o(t) = \frac{|s_i(t)|}{\left[1 + \left(\frac{|s_i(t)|}{q}\right)^{2v}\right]^{\frac{1}{2v}}} e^{j\phi(t)}, \tag{34}$$

where $s_i(t) = x(t)e^{j\phi(t)}$ is the input signal and $s_o(t)$ is the output of SSPA. We set SSPA parameters v and q as 3 and 1dB, respectively. The CR is set to 5.5dB for the OICF, ICF, SCF and TKM-ICF methods with only one iteration. The original OFDM signal without any PAPR reduction technique is also included. The power spectrum density (PSD) of SSPA's output is shown in Fig. 8, which are evaluated by averaging several periodogram estimates. It can be seen that the original OFDM signal leads to large out-of-band radiation compared with those using PAPR reduction techniques. All these clipping and filtering methods can bring better performance of out-of-band radiation at different level. We can observe that the OICF method achieves the lowest out-of-band radiation and the TKM-ICF method also brings about negligible performance difference to the OICF method.

V. CONCLUSIONS AND FUTURE WORK

In this paper, a new ICF method based on the time-domain kernel matrix has been proposed. Instead of frequency filtering, the PAPR-reduction signal is generated to approximate the clipping noise by constructing a time-domain kernel matrix and optimizing the corresponding scaling vector. According to the statistical analysis, we sort the observation of clipping noise into three cases and simplify the problem into several sub-problem. By using the curve fitting procedure, the proposed method can adapt to different PAPR requirements. The simulation results show that the proposed TKM-ICF method has near optimal performance in terms of PAPR reduction and EVM. Meanwhile, it is also demonstrated that the TKM-ICF method is more efficient to achieve the desired PAPR than the other iterative clipping and filtering methods.

Future work will focus on the performance of proposed method with some new OFDM-based waveforms, such as WOLA-OFDM, filtered-OFDM and FBMC. Because of the severe suppression of the out-of-band radiation using additional windowing and filtering operations, the PAPR-reduction signal should be redesigned to satisfy the requirement of spectrum confinement. Future study will also address the optimization problem formulation that contains both PAPR reduction and the suppression of power leakage, and the intuitive method that has significantly reduced complexity. The adjacent channel interference is also to be considered with the PAPR reduction for the sake of improving the capacity of adjacent channel co-existence which is of prime importance in future mobile communication systems.

REFERENCES

[1] Y. Rahmatallah and S. Mohan, "Peak-to-average power ratio reduction in OFDM systems: A survey and taxonomy," *IEEE Commun. Surveys Tuts.*, vol. 15, no. 4, pp. 1567–1592, Nov. 2013.
[2] T. Jiang and Y. Wu, "An overview: Peak-to-average power ratio reduction techniques for OFDM signals," *IEEE Trans. Broadcast.*, vol. 54, no. 2, pp. 257–268, Jun. 2008.
[3] J. Tellado and J. M. Cioffi, "Peak power reduction for multicarrier transmission," in *Proc. IEEE GLOBECOM*, vol. 99, Dec. 1999, pp. 5–9.
[4] R. W. Bäuml, R. F. H. Fischer, and J. B. Huber, "Reducing the peak-to-average power ratio of multicarrier modulation by selected mapping," *Electron. Lett.*, vol. 32, no. 22, pp. 2056–2057, Oct. 1996.
[5] S. H. Müller and J. B. Huber, "OFDM with reduced peak-to-average power ratio by optimum combination of partial transmit sequences," *Electron. Lett.*, vol. 33, no. 5, pp. 368–369, Feb. 1997.
[6] K. Anoh, B. Adebisi, M. Rabie, and C. Tanriover, "Root-based nonlinear companding technique for reducing PAPR of precoded OFDM signals," *IEEE Access*, vol. 6, pp. 4618–4629, 2018.
[7] J. Armstrong, "Peak-to-average power reduction for OFDM by repeated clipping and frequency domain filtering," *Electron. Lett.*, vol. 38, no. 5, pp. 246–247, Feb. 2002.
[8] L. Wang and C. Tellambura, "A simplified clipping and filtering technique for PAR reduction in OFDM systems," *IEEE Signal Process. Lett.*, vol. 12, no. 6, pp. 453–456, Jun. 2005.
[9] I. Sohn and S. C. Kim, "Neural network based simplified clipping and filtering technique for PAPR reduction of OFDM signals," *IEEE Commun. Lett.*, vol. 19, no. 8, pp. 1438–1441, Aug. 2015.
[10] R. J. Baxley, C. Zhao, and G. T. Zhou, "Constrained clipping for crest factor reduction in OFDM," *IEEE Trans. Broadcast.*, vol. 52, no. 4, pp. 570–575, Dec. 2006.
[11] S. K. Deng and M. C. Lin, "Recursive clipping and filtering with bounded distortion for PAPR reduction," *IEEE Trans. Commun.*, vol. 55, no. 1, pp. 227–230, Jan. 2007.
[12] Y.-C. Wang and Z.-Q. Luo, "Optimized iterative clipping and filtering for PAPR reduction of OFDM signals," *IEEE Trans. Commun.*, vol. 59, no. 1, pp. 33–37, Jan. 2011.
[13] X. Zhu, W. Pan, H. Li, and Y. Tang, "Simplified approach to optimized iterative clipping and filtering for PAPR reduction of OFDM signals," *IEEE Trans. Commun.*, vol. 61, no. 5, pp. 1891–1901, May 2013.
[14] K. Anoh, C. Tanriover, and B. Adebisi, "On the optimization of iterative clipping and filtering for PAPR reduction in OFDM systems," *IEEE Access*, vol. 5, pp. 12004–12013, 2017.
[15] A. M. Rateb and M. Labana, "An optimal low complexity PAPR reduction technique for next generation OFDM systems," *IEEE Access*, vol. 7, pp. 16406–16420, 2019.
[16] K. Anoh, C. Tanriover, B. Adebisi, and M. Hammoudeh, "A new approach to iterative clipping and filtering PAPR reduction scheme for OFDM systems," *IEEE Access*, vol. 6, pp. 17533–17544, 2018.
[17] A. Saul, "Generalized active constellation extension for peak reduction in OFDM systems," in *Proc. IEEE ICC*, vol. 3, Seoul, Korea, May 2005, pp. 1974–1979.

[18] H. Ochiai and H. Imai, "On the distribution of the peak-to-average power ratio in OFDM signals," *IEEE Trans. Commun.*, vol. 49, no. 2, pp. 282–289, Feb. 2001.
[19] L. Wang and C. Tellambura, "Analysis of clipping noise and tone-reservation algorithms for peak reduction in OFDM systems," *IEEE Trans. Veh. Technol.*, vol. 57, no. 3, pp. 1675–1694, May 2008.
[20] H. Li, T. Jiang, and Y. Zhou, "An improved tone reservation scheme with fast convergence for PAPR reduction in OFDM systems," *IEEE Trans. Broadcast.*, vol. 57, no. 4, pp. 902–906, Dec. 2011.
[21] T. Jiang, C. Ni, C. Xu, and Q. Qi, "Curve fitting based tone reservation method with low complexity for PAPR reduction in OFDM systems," *IEEE Commun. Lett.*, vol. 18, no. 5, pp. 805–808, May 2014.
[22] P. Yu and S. Jin, "A low complexity tone reservation scheme based on time-domain kernel matrix for PAPR reduction in OFDM systems," *IEEE Trans. Broadcast.*, vol. 61, no. 4, pp. 710–716, Dec. 2015.
[23] C. Tellambura, "Computation of the continuous-time PAR of an OFDM signal with BPSK subcarriers," *IEEE Commun. Lett.*, vol. 5, no. 5, pp. 185–187, May 2001.
[24] M. Grant and S. Boyd. (Oct. 2008). *CVX: MATLAB Software for Disciplined Convex Programming (Web Page and Software)*. [Online]. Available: http://stanford.edu/ boyd/cvx
[25] H. Guo and C. S. Burrus, "Wavelet transform based fast approximate Fourier transform," in *Proc. IEEE ICASSP*, vol. 3, Apr. 1997, pp. 1973–1976.

XIAORAN LIU received the B.S. and M.S. degrees from the National University of Defense Technology, Changsha, China, in 2014 and 2016, respectively, where he is currently pursuing the Ph.D. degree with the School of Electronic Science. His research interests include wireless communications technology, optimization method, and 5G technology.

XIAOYING ZHANG received the M.S. and Ph.D. degrees in communication engineering from the National University of Defense Technology (NUDT), Changsha, China, in 2002 and 2008, respectively. From 2007 to 2008, she was a Visiting Scholar with Kyushu University, Japan. Since 2014, she has been an Associate Professor with NUDT. From 2017 to 2017, she was a Visiting Scholar with the 5G Innovation Centre (5GIC), Institute of Communications, University of Surrey, U.K. Her main research interests include wireless communications, new air interface design, receiver design, and iterative signal processing for wireless communication systems.

JUN XIONG received the B.S. and Ph.D. degrees from the National University of Defense Technology (NUDT), Changsha, China, in 2009 and 2014, respectively, where he is currently a Lecturer with the School of Electronic Science. His research interests include cooperative communications, physical-layer security, and resource allocation.

FANGLIN GU received the B.S. degree in communication engineering and the Ph.D. degree in information and communication engineering from the PLA University of Science and Technology, Nanjing, China, in 2008 and 2013, respectively. He is currently a Lecturer with the Communication Engineering Department, National University of Defense Technology, Changsha, China. His research interest includes the areas of signal processing for communications.

JIBO WEI received the B.S. and M.S. degrees in electronic engineering from the National University of Defense Technology, Changsha, China, in 1989 and 1992, respectively, and the Ph.D. degree in electronic engineering from Southeast University, Nanjing, China, in 1998. His research interests include wireless network protocol and signal processing in communications, more specially, the areas of multicarrier transmission, cooperative communication, and cognitive networks.